

Synthesis of small silver nanocubes in a hydrophobic solvent by introducing oxidative etching with Fe(III) species†

Yanyun Ma,^{ab} Weiyang Li,^a Jie Zeng,^a Maureen McKiernan,^c Zhaoxiong Xie^b and Younan Xia^{*a}

Received 27th January 2010, Accepted 23rd March 2010

First published as an Advance Article on the web 9th April 2010

DOI: 10.1039/c0jm00187b

The role of oxidative etching in the synthesis of noble-metal nanocrystals with a hydrophilic solvent (in particular, ethylene glycol) has been explored in our previous work. In this paper, we demonstrate that the mechanism of oxidative etching could be extended to the synthesis of single-crystal Ag nanocrystals in a hydrophobic solvent such as isoamyl ether. In this case, Fe(III) species in the form of FeCl₃ or Fe(acac)₃ had to be introduced into the hydrophobic system as an effective etching agent. The final product contained single-crystal Ag nanocubes (slightly truncated) with an edge length as small as ~13.5 nm, a size that has been difficult to achieve using a hydrophilic system.

Over the past decade, Ag nanostructures have received considerable attention owing to one of their remarkable properties known as localized surface plasmon resonance (LSPR), which has enabled a rich variety of applications, including their use as optical probes, contrast agents, sensors, plasmonic waveguides, and substrates for surface enhanced Raman scattering (SERS).^{1–8} With respect to synthesis, it is difficult to produce single-crystal Ag nanostructures with well-defined shapes in high yields because Ag has a strong tendency to form twinned structures at small sizes.⁹ As a result, the synthesis is typically dominated by twinned seeds (with all possible numbers of twin defects) at early stages and irregular particles with poorly defined shapes in the product. This situation did not change until our group demonstrated a polyol reduction method for the synthesis of single-crystal Ag nanocubes in a hydrophilic solvent, ethylene glycol (EG), with the help of poly(vinyl pyrrolidone) (PVP), a capping agent that binds selectively to the {100} facets.¹⁰

In a hydrophilic solvent such as water or EG, oxidative etching (a process similar to corrosion) has been effectively employed to control the number of twin defects in the seeds and thereby facilitate the preferential formation of Ag nanostructures with specific shapes or morphologies.^{9,11–15} Due to the presence of defects on the surface of twinned seeds, they are more susceptible to oxidative etching than their single-crystal counterparts. As a result, only single-crystal seeds can survive and further grow into single-crystal nanostructures such

as cubes and octahedrons. To oxidize zero-valent metal atoms to ions, a wet etchant typically must contain both an oxidant (*e.g.*, the O₂ from air) and a ligand (*e.g.*, Cl[–] ions added in the form of NaCl or HCl) that can coordinate to the metal ions.^{9,16} In addition, iron species, either Fe(III) or Fe(II), has been found to be a good source of etchants for removing twinned seeds and promoting the formation of single-crystal Ag nanostructures.¹³

The present work is based upon the notion that oxidative etching might be extendable to a hydrophobic system, such as a conventional organic solvent, and thus provide a facile method for the synthesis of single-crystal Ag nanostructures. One of the biggest advantages for making metal nanocrystals in a hydrophobic solvent is that monodisperse samples with greatly reduced sizes can be generated, which is of great importance in developing highly active and selective catalysts. For example, Yin and co-workers demonstrated the synthesis of monodisperse Ag nanospheres (11 nm in size) using 1,2-hexadecanediol as a reducing agent and oleylamine as a surfactant in *o*-dichlorobenzene at 180 °C.¹⁷ However, the exact mechanism of this synthesis is yet to be uncovered. It is also not clear if this method can be applied to the synthesis of faceted Ag nanocrystals with sizes approaching 10 nm. It is worth pointing out that it has been very difficult to obtain Ag nanocubes with edge lengths smaller than 25 nm *via* the hydrophilic system based on polyol reduction.^{18,19} Herein, we demonstrate an effective approach to the synthesis of Ag nanocubes (with slight truncation) as small as 13.5 nm in edge length using a modified thermal decomposition method in a hydrophobic system, in which a trace amount of Fe(III) species was added as an effective etchant.

We first conducted the synthesis without the involvement of oxidative etching. Silver trifluoroacetate was used as a silver precursor and decomposed in isoamyl ether at 150 °C in the presence of oleylamine as a capping agent under the protection of argon gas. This is similar to the protocol reported by Yang and coworkers.²⁰ In a typical procedure, 0.22 g silver trifluoroacetate, 0.66 mL oleylamine, and 10 mL isoamyl ether were mixed in a 3-neck flask and the flask was heated from room temperature to 150 °C within 60 min in an oil bath while the reaction solution was continuously bubbled with argon gas. The reaction was continued at 150 °C for another 100 min, and a solution with a brownish color was obtained, indicating the formation of Ag nanoparticles. After centrifugation and washing with acetone and hexane, the product was collected and re-dispersed in hexane. Fig. 1A shows a typical transmission electron microscopy (TEM) image of the as-prepared sample. It can be observed that the Ag nanocrystals prepared using this procedure had a relatively narrow size distribution. Fig. 1B shows a TEM image at a higher magnification, indicating that the nanocrystals had a diameter of approximately 14 nm. The high-resolution TEM image (Fig. 1C)

^aDepartment of Biomedical Engineering, Washington University, St. Louis, Missouri, 63130, USA. E-mail: xia@biomed.wustl.edu; Fax: +1 314-935-7448; Tel: +1 314-935-8328

^bState Key Laboratory for Physical Chemistry of Solid Surfaces, Department of Chemistry, College of Chemistry and Chemical Engineering, Xiamen University, Xiamen, Fujian, 361005, P. R. China

^cDepartment of Chemistry, Washington University, St. Louis, Missouri, 63130, USA

† Electronic supplementary information (ESI) available: TEM images Fig. S1–S3. See DOI: 10.1039/c0jm00187b

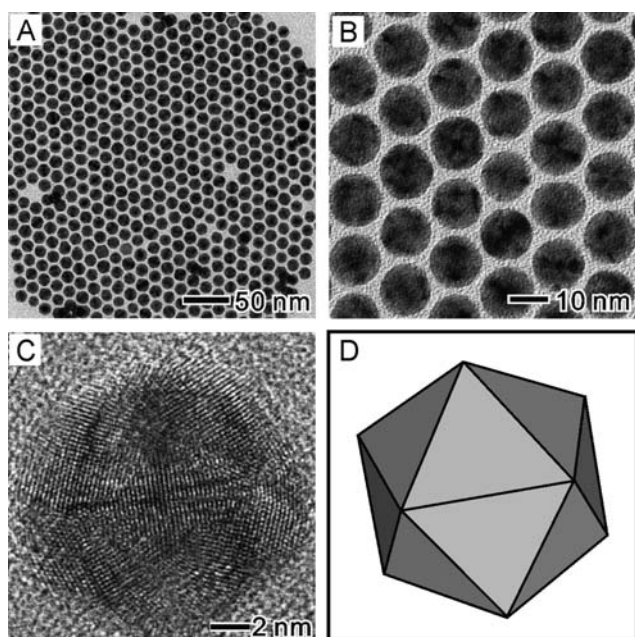


Fig. 1 (A and B) TEM images with different magnifications of the Ag nanocrystals prepared under argon protection in a 3-neck flask at 150 °C for 100 min. The average diameter of the Ag nanocrystals was 14 nm. (C) A high-resolution TEM image of a nanocrystal from the same sample, revealing the multiply-twinned structure that matches an icosahedron. (D) The corresponding geometrical model of an icosahedron with roughly the same orientation as the one shown in (C).

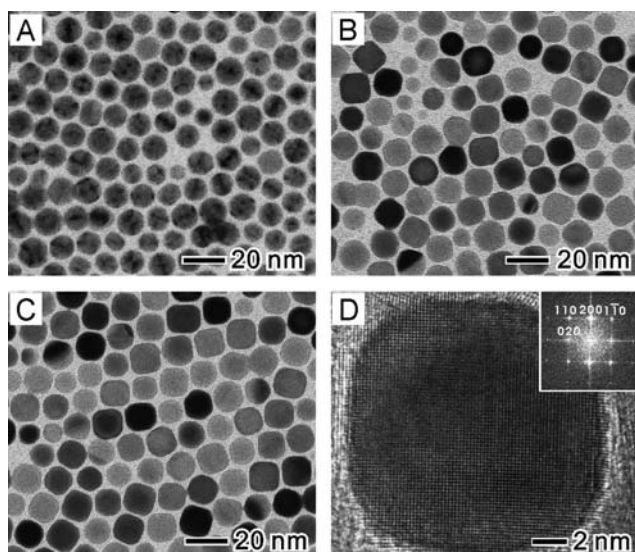


Fig. 2 TEM images of Ag nanocrystals prepared without the protection of argon gas under different conditions: (A) in air, (B and C) in air and in the presence of (B) Fe(acac)₃ and (C) FeCl₃, respectively. In the presence of Fe(III) species, the products became single-crystal nanocubes with edge length around 13.5 nm. (D) A high-resolution TEM image of an individual Ag nanocube shown in (C), indicating that it was a single crystal. The inset is the corresponding FFT pattern, showing symmetrical spots which can be indexed as {200} and {110} reflections of *fcc* silver.

taken from an individual particle reveals a multiply-twinned structure, which can be related to icosahedron. Fig. 1D shows a corresponding geometrical model of an icosahedron with roughly the same orientation as the one shown in Fig. 1C.

Fig. 2A shows a typical TEM image of the as-prepared Ag sample synthesized under experimental conditions similar to those for the sample shown in Fig. 1, except that the reaction was performed in air instead of under argon protection. It is clear that a great majority of the product still had a multiply-twinned structure in the shape of icosahedron with the rare exception of a few single-crystal nanocrystals. These nanocrystals had an average diameter of 13 nm, albeit their size distribution was not as narrow as that for the sample obtained under argon protection. Overall, no significant change to crystallinity and shape was observed when the reaction was performed in air, indicating that the O₂ from air alone could not completely etch away the twinned seeds in the early stage of the synthesis. It is clear that we need to add an extra reagent. However, we found that NaCl, which is usually used as an etching agent (when combined with the O₂ from air) in a hydrophilic system, cannot be dissolved in isoamyl ether.

To solve the solubility problem, we introduced the Fe(III) species, which could serve as a dual etchant for the formation of single-crystal Ag nanocrystals. In a typical synthesis, 0.1 mmol silver trifluoroacetate, 0.2 mmol oleylamine, and 4.5 mL isoamyl ether were mixed in a flask placed in an oil bath and heated at 100 °C for 20 min. We then added 1 μmol FeCl₃ or Fe(acac)₃ in 0.5 mL isoamyl ether to the mixture under magnetic stirring and the flask was quickly transferred to another oil bath held at 150 °C. After the reaction proceeded for another 60 min, the mixture was cooled down to room temperature naturally. The product was collected by centrifugation, washed with acetone and hexane twice, and finally re-dispersed in hexane. Fig. 2B and C, show TEM images of Ag nanocrystals obtained by adding trace amounts of Fe(acac)₃ and FeCl₃, respectively, into the reaction system. In both cases, single-crystal Ag nanocubes with slight truncation could be obtained. Compared to the case of Fe(acac)₃ (Fig. 2B), the yield of Ag nanocubes increased from ~55% to ~70% when FeCl₃ was used as an etchant (Fig. 2C). This could be explained by a stronger etching power from both Fe(III) species and Cl⁻ in the case of FeCl₃. Fig. S1† shows a low-magnification TEM image of the sample in Fig. 2C, indicating good uniformity of this sample. In addition, TEM images (Fig. S2†) of three Ag nanocrystals at different orientations and different tilting angles (0°, 30° and 56°) clearly indicate that they were cubic structures rather than square-shaped plates (the projection of a plate should be rod-like when tilted at 56°). In addition, some spherical-like particles shown in Fig. 2C are actually truncated cubes projected from a specific orientation (see Fig. S2†). The nanocubes shown in Fig. 2C were ~13.5 nm in edge length. The corners (and probably edges) of the Ag nanocubes were slightly truncated because the atoms at the corners of a nanocube are higher in free energy, making them unstable in an oxidative environment. Fig. 2D shows a typical high-resolution TEM image of an individual Ag nanocube shown in Fig. 2C, where the well-resolved and continuous fringes indicate that it was a single crystal. In the corresponding fast Fourier transform (FFT) pattern (inset of Fig. 2D), the spots could be indexed to the {200} and {110} reflections of face-centered cubic (*fcc*) silver.

To understand the mechanism responsible for the formation of single-crystal nanocubes shown in Fig. 2C, we monitored the synthesis by taking aliquots of the reaction mixture at different time

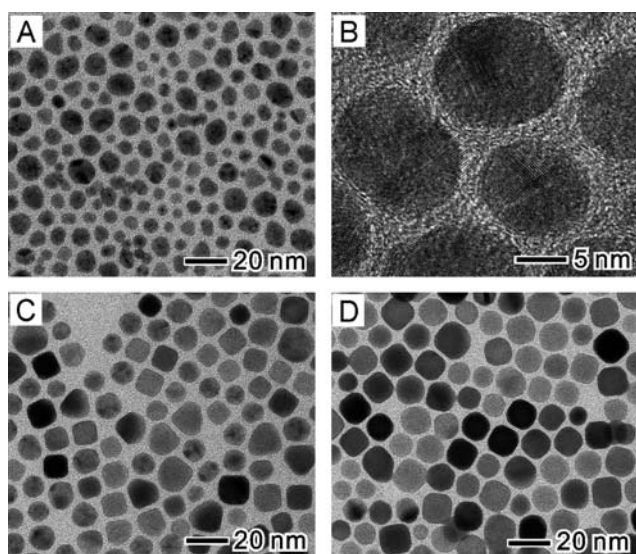
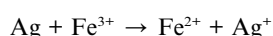


Fig. 3 TEM images of Ag nanocrystals taken at (A) 10, (C) 15, and (D) 60 min after the addition of FeCl₃ (1 μmol, Ag(I) : Fe(III) = 100 : 1). (B) A high-resolution TEM image of the Ag nanocrystals in (A), showing the twinned structures of Ag nanocrystals in the early stage.

points and then analyzing them by TEM. As shown in Fig. 3A, many irregularly shaped nanocrystals were obtained at $t = 10$ min. The high-resolution TEM image in Fig. 3B reveals that most of the nanoparticles formed at early stages exhibit a multiply-twinned structure (only a few of them were single-crystal, as shown in Fig. S3[†]). As the reaction proceeded to $t = 15$ min, the amount of twinned particles decreased and single-crystal particles with a more or less cubic shape appeared (Fig. 3C). As the reaction time was further extended to $t = 60$ min, essentially all the particles were single-crystal cubes with slight truncation (Fig. 3D). On the basis of these observations, it is obvious that the single-crystal Ag nanocubes in the final product were derived from the twinned particles formed in the early stage of the reaction. As the reaction proceeded, the defect regions inherently present on twinned seeds are much higher in activity relative to the single-crystal regions and thus were preferentially etched and oxidized back to Ag(I) by Fe(III) which was simultaneously reduced to Fe(II), as shown in following equation.²¹



The resultant Ag⁺ ions were then reduced again by oleylamine on the surface of pre-existing single-crystal Ag seeds, resulting in a continuous, epitaxial growth of twin-free nanocrystals. The Fe(II) could be quickly and easily oxidized back to Fe(III) by the O₂ from air. The continuous etching and re-growth, accompanied by the redox cycle of Fe(III)/Fe(II), converted the nanocrystals from multiply-twinned to single-crystal species.

We also found that the amount of FeCl₃ in the reaction solution played a critical role in the formation of Ag nanocrystals. Fig. 4A shows TEM image of the as-prepared sample when a reduced amount of FeCl₃ (0.1 μmol rather than 1 μmol) was added to the reaction solution. In this case, both single-crystal and multiply-twinned nanocrystals were obtained with sizes varying in the range of 5–12 nm. This can be explained by the insufficient amount of etchant,

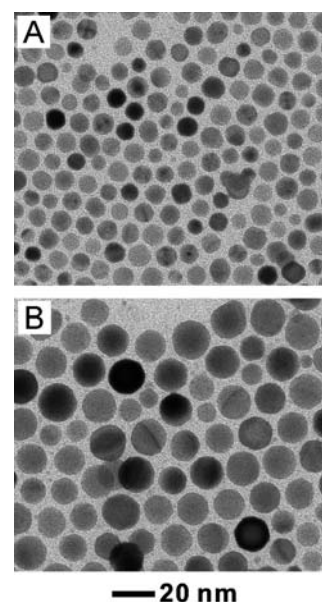


Fig. 4 TEM images of samples taken from two reactions at $t = 60$ min. The reactions contained (A) 0.1 μmol and (B) 10 μmol of FeCl₃, respectively, while other parameters were the same as those used in Fig. 2C.

which led to the insufficient etching of twinned seeds in the early stages of the reaction. In contrast, when the amount of FeCl₃ added into the reaction was increased to 10 μmol, single-crystal spherical particles (rather than a cubic shape) with sizes in the range of 10–19 nm were formed, as shown in Fig. 4B. This might be due to the increased etching power which caused further truncation for the nanocubes. In addition, the excess amount of FeCl₃ could etch not only the multiply-twinned seeds at early stages, but also part of the single-crystal seeds. Therefore, fewer seeds were formed, and thus the particles grew bigger when the reaction time was kept the same as the samples shown in Fig. 4A and Fig. 2C. In addition, the very small portion of singly-twinned nanocrystals shown in Fig. 4B might be due to salt-induced dimerization of single-crystal seeds, a process commonly occurs at increased concentrations for the salt.⁸

In summary, we have successfully demonstrated the synthesis of single-crystal Ag nanocubes (with slight truncation) of around 13.5 nm in edge length by thermal decomposition of silver trifluoroacetate in isoamyl ether in the presence of oleylamine. A trace amount of Fe(III) species such as FeCl₃ or Fe(acac)₃ was added into the reaction, serving as an effective etchant to control the crystallinity and shape of the resultant Ag nanocrystals. By monitoring the etching process with aliquots taken from the reaction at different time points, it was clear that the addition of Fe(III) species resulted in preferential etching of twinned seeds at early stages, leaving behind only the single-crystal seeds to grow. These results reveal that the oxidative etching mechanism not only works for a hydrophilic system (water or EG), but can also be extended to a hydrophobic system (organic solvent). It was also found that the degree of etching and the size/shape of the resultant Ag nanocrystals mainly depended on the amount of etchant added.

Acknowledgements

This work was supported in part by the NSF (DMR-0804088) and an NIH Director's Pioneer Award (DPI OD000798). Part of the work

was performed in the Nano Research Facility (NRF), a member of the National Nanotechnology Infrastructure Network (NNIN), which is supported by the National Science Foundation under NSF award no. ECS-0335765. Y.M. would like to acknowledge a partial financial support from the China Scholarship Council.

Notes and references

- 1 Y. C. Cao, R. Jin and C. A. Mirkin, *Science*, 2002, **297**, 1536–1540.
- 2 A. P. Alivisatos, *Nat. Biotechnol.*, 2004, **22**, 47–52.
- 3 A. L. Pyayt, B. Wiley, Y. Xia, A. Chen and L. Dalton, *Nat. Nanotechnol.*, 2008, **3**, 660–665.
- 4 P. L. Stiles, J. A. Dieringer, N. L. Shah and R. P. Van Duyne, *Annu. Rev. Anal. Chem.*, 2008, **1**, 601–626.
- 5 M. J. Banholzer, J. E. Millstone, L. Qin and C. A. Mirkin, *Chem. Soc. Rev.*, 2008, **37**, 885–897.
- 6 C. M. Copley, M. Rycenga, F. Zhou, Z. Li and Y. Xia, *J. Phys. Chem. C*, 2009, **113**, 16975–16982.
- 7 B. J. Wiley, S. H. Im, Z. Li, J. McLellan, A. Siekkinen and Y. Xia, *J. Phys. Chem. B*, 2006, **110**, 15666–15675.
- 8 W. Li, P. H. C. Camargo, X. Lu and Y. Xia, *Nano Lett.*, 2009, **9**, 485–490.
- 9 B. Wiley, T. Herricks, Y. Sun and Y. Xia, *Nano Lett.*, 2004, **4**, 1733–1739.
- 10 Y. Sun and Y. Xia, *Science*, 2002, **298**, 2176–2179.
- 11 C. M. Copley, M. Rycenga, F. Zhou, Z. Y. Li and Y. Xia, *Angew. Chem., Int. Ed.*, 2009, **48**, 4824–4827.
- 12 C. Xue, G. S. Metraux, J. E. Millstone and C. A. Mirkin, *J. Am. Chem. Soc.*, 2008, **130**, 8337–8344.
- 13 B. Wiley, Y. Sun and Y. Xia, *Langmuir*, 2005, **21**, 8077–8080.
- 14 Y. Xiong, J. Chen, B. Wiley, Y. Xia, S. Aloni and Y. Yin, *J. Am. Chem. Soc.*, 2005, **127**, 7332–7333.
- 15 J. Chen, T. Herricks and Y. Xia, *Angew. Chem., Int. Ed.*, 2005, **44**, 2589–2592.
- 16 J. Chen, J. M. McLellan, A. Siekkinen, Y. Xiong, Z. Li and Y. Xia, *J. Am. Chem. Soc.*, 2006, **128**, 14776–14777.
- 17 Y. Yin, C. Erdonmez, S. Aloni and A. P. Alivisatos, *J. Am. Chem. Soc.*, 2006, **128**, 12671–12673.
- 18 A. R. Siekkinen, J. M. McLellan, J. Chen and Y. Xia, *Chem. Phys. Lett.*, 2006, **432**, 491–496.
- 19 Q. Zhang, C. M. Copley, L. Au, M. McKiernan, A. Schwartz, J. Chen, L. Wen and Y. Xia, *ACS Appl. Mater. Interfaces*, 2009, **1**, 2044–2048.
- 20 X. Z. Lin, X. Teng and H. Yang, *Langmuir*, 2003, **19**, 10081–10085.
- 21 X. Lu, L. Au, J. McLellan, Z. Y. Li, M. Marquez and Y. Xia, *Nano Lett.*, 2007, **7**, 1764–1769.